Catalysis Today 148 (2009) 184–188

Contents lists available at ScienceDirect

Catalysis Today

journal homepage: www.elsevier.com/locate/cattod

Aminopropyl-functionalized silicas synthesized by W/O microemulsion for immobilization of penicillin G acylase

Bianfang Shi, Yunsong Wang, Yanglong Guo *, Yanqin Wang, Ying Wang, Yun Guo, Zhigang Zhang, Xiaohui Liu, Guanzhong Lu *

Lab for Advanced Materials, Research Institute of Industrial Catalysis, East China University of Science and Technology, Shanghai 200237, PR China

ARTICLE INFO

Article history:
Available online 21 March 2009

Keywords:
Aminopropyl-functionalized silicas
Microemulsion
Immobilization
Penicillin G acylase

ABSTRACT

The aminopropyl-functionalized silicas (APFS) with higher loading of amino groups was synthesized by the co-condensation of tetraethylorthosilicate (TEOS) and γ-aminopropyltriethoxysilane (APTES) in W/O microemulsion. Thus synthesized APFS was characterized by FT-IR spectroscopy, thermogravimetry, element analysis, solid state ^{13}C and ^{29}Si MAS NMR, TEM, and N_2 sorption. The results show that the aminopropyl groups were condensed as the part of the silicate framework, and the amino contents could be adjusted by changing the volume ratio of APTES to TEOS in W/O microemulsion. APFS has been firstly used as the support for the immobilization of penicillin G acylase after activation with glutaraldehyde. Effects of the volume ratio of APTES to TEOS on the physico-chemical properties of APFS and the performance of immobilized penicillin G acylase were systematically investigated. Penicillin G acylase immobilized on APFS with the volume ratio of APTES/TEOS = 1/9 (1.77 mmol g^{-1} amino groups) behaves higher specific activity of 2759 IU g^{-1} and higher operational stability of 86% of the initial specific activity after recycled for 5 times, and the immobilization yield of 97%.

1. Introduction

Enzyme immobilized on the insoluble carriers with physical forces or covalent bonding is gaining importance in many industrial and biomedical applications because of its reusability and easy separation. Penicillin G acylase (PGA), which has been one of the most important industrial biocatalysts since its discovery in 1960, is widely used in the production of 6-aminopenicillanic acid (6-APA), 7-aminodeacetoxycephalosporanic acid (7-ADCA), and the semi-synthetic β-lactam antibiotics [1]. However, its dissolubility is the main obstacle in the industrial applications. Therefore an efficient recovery and reuse of PGA is a prerequisite for its economic industrial applications. To immobilize PGA on a solid support is a good solution and has attracted much attention. The key factor of enzyme immobilization is the choice of carriers. Many carriers, both organic and inorganic, such as resins, magnetic microparticles of polymers, layered double hydroxides (LDH), mesoporous silicas, and so on, have been used for the immobilization of PGA. Organic polymeric carriers are the most widely studied materials because of the presence of rich functional groups, which provide the essential interactions with the enzymes. For example, Lu's group [2,3] and other groups [4,5] have used oxirane acrylic beads as an enzyme carrier. However, organic materials have a low reusability and create the problems in disposal. Nowadays inorganic materials, such as mesoporous silicas, have been excessively studied by many groups [6–9] because they are thermally and mechanically stable, environmentally friendly, and highly resistant against microbial attacks and organic solvents.

Silica materials have many applications in the areas including composite materials, photonics, thermal insulators, sensors, catalysts, adsorbents, immunoassays, and so on. The organic functionalization of silica materials can expand the applications in many aspects and control the overall properties of the materials for the desired applications. Nature of the functional groups on the silica surface usually plays a critical role in the surface properties, such as chemical reactivity and hydrophobicity [10]. γ-Aminopropyl groups loaded on the silica surface are important groups because they have many applications, such as covalent coupling of protein to the surface of the silica materials [11], base adsorbent for carbon dioxide [12], ligand groups for some heavy metals and metal salts, base solid catalysts for heterogeneous reactions [13–15] and supports for some catalysts [16–20]. The organic group-functionalized silicas can be prepared by two methods, such as grafting method (post-modification) and co-condensation method [21–23]. Grafting method, which carried out by a reaction of a suitable organosilane with the surface silanol groups, is firstly used to modify amorphous silicas or mesoporous silica materials. However, there are two main shortcomings: one is the limited

* Corresponding authors. Tel.: +86 21 64252923; fax: +86 21 64252923.
E-mail addresses: ylguo@ecust.edu.cn (Y. Guo), gzhlu@ecust.edu.cn (G. Lu).

0920-5861/$ – see front matter © 2009 Elsevier B.V. All rights reserved.
doi:10.1016/j.cattod.2009.02.014

loading level and the inhomogeneous distribution of the functional groups, the other is the complicated procedure. The co-condensation method, which is usually used in the synthesis of organic group-functionalized mesoporous silicas, can solve the above problems, which can offer higher and more uniform surface coverage of the functional groups. Recently, aminopropyl-functionalized mesoporous silicas [14,24,25] has been prepared with the co-condensation of tetraethylorthosilicate (TEOS) and γ-aminopropyltrialkoxysilane, while higher loading of organic groups can destroy the ordering of the mesostructures. Furthermore, the removal of the template in mesoporous silicas is a challenge because of the low thermal stability of organic groups, which cannot be removed by calcination. Microemulsion method may be a good choice to synthesize organic group-functionalized silicas by co-condensation because the surfactants and organic solvent can be washed easily, more important, the loading of amino groups can be higher. The density of amino groups loading on the silica surface can influence the chemical reactivity and the binding capability.

In this paper, a novel and facile route was developed to synthesize the aminopropyl-functionalized silicas (APFS), one-pot synthesized by the co-condensation of tetraethylorthosilicate and γ-aminopropyltriethoxysilane (APTES) in W/O microemulsion and then used as the carrier for PGA immobilization, which have not yet been reported. The higher specific activity of immobilized PGA was obtained when compared with other aminopropyl-functionalized silica materials [7,9,26]. Furthermore, effects of the volume ratio of APTES to TEOS on the physico-chemical properties of APFS and the performance of immobilized PGA (IMPGA) were systematically investigated. The procedure for preparation of APFS and immobilization of PGA was shown in Scheme 1.

2. Experimental

2.1. Chemicals

γ-Aminopropyltriethoxysilane was purchased from Aldrich. Penicillin G acylase (804 IU/mL) was purchased from Zhejiang Hiader Co. Ltd. Penicillin G potassium salt was bought from Shandong Lukang Pharmaceutical Co. Ltd. Tetraethylorthosilicate and glutardialdehyde were bought from Shanghai Sinopharm Chemical Reagent Co. Ltd. Triton X-100, *n*-hexanol and cyclohexane were analytical grade and used without further purification. NaOH aqueous solution and phosphate buffers were prepared according to the reference [9].

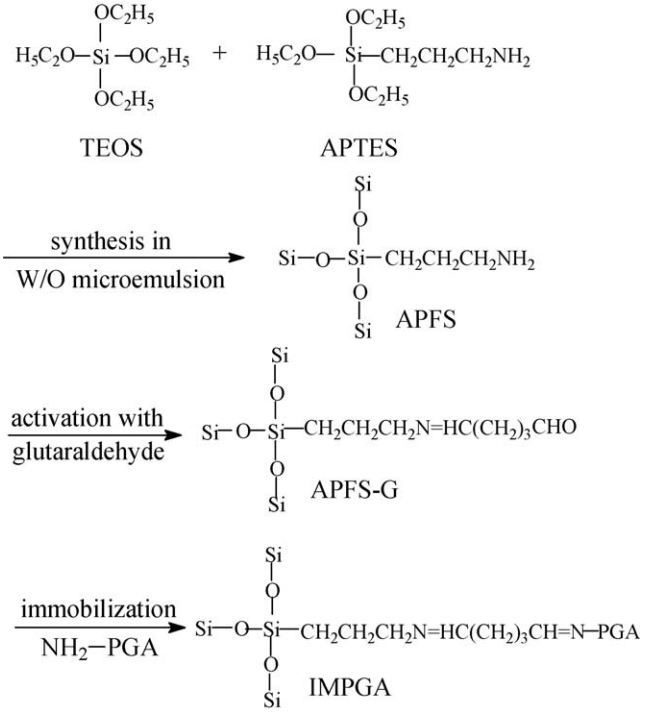

Scheme 1. The procedure for preparation of APFS and immobilization of PGA.

2.2. Synthesis of aminopropyl-functionalized silicas

The aminopropyl-functionalized silicas was synthesized in a W/O microemulsion. A typical procedure for the preparation of W/O microemulsion was described as follows: first, 12 mL Triton X-100 and 12 mL *n*-hexanol were added to cyclohexane, and then the mixture was stirred for 5 min to obtain the external oil phase. The aqueous phase of 10 mL 0.25 mol L^{-1} ammonium hydroxide was added to the external oil phase and kept stirring for 15 min to obtain W/O microemulsion. In this W/O microemulsion, 5 mL TEOS was added and stirred for 30 min, and then 5 mL APTES was added to the mixture. The hydrolysis and co-condensation of TEOS with APTES was done for 22 h with gently stirring. After reaction, the mixture was filtered and washed with acetone, then dried at room temperature under vacuum. The volume ratio of APTES to TEOS was changed and the samples were denoted as APFS-*x*-*y*, *x* represents the volume of APTES, *y* represents the volume of TEOS, the total volume of *x* and *y* should be kept in 10 mL.

2.3. Immobilization of PGA on APFS

2.3.1. Activation of APFS with glutaraldehyde

0.5 g APFS was added to 5.7 mL pH 8.0 phosphate buffer, then 2.3 mL glutaraldehyde was added to the above mixture under the atmosphere of N_2, the mixture was sealed and stirred at 30 °C for 2 h. After filtration and extensive washing with the deionized water, the resulted samples are denoted as APFS-*x*-*y*-G and are used to immobilize PGA.

2.3.2. Immobilization of PGA

0.5 g activated sample was mixed with 6 mL PGA aqueous solution which was diluted with 0.1 mol L^{-1} pH 8.0 phosphate buffer (V_{enzyme}/V_{buffer} = 1/2). The mixture of APFS-*x*-*y*-G and PGA solution was stirred at 130 rpm at 30 °C for 24 h. Then the mixture was filtered and washed with 400 mL deionized water for many times. The resulting IMPGA was placed in the refrigerator at 4 °C for the subsequent activity assays.

2.4. Activity assays of IMPGA

The specific activity of IMPGA was determined by titrating phenylacetic acid (PAA) with NaOH aqueous solution, which is a by-product in the hydrolysis reaction of penicillin G potassium salt [3].

The procedure of determining the specific activity of IMPGA was as follows: 0.15 g wet IMPGA, 12 mL deionized water and 3 mL phosphate buffer (0.1 mol L^{-1}, pH 8.0) were mixed homogenously and kept at 37 °C in the thermostatic water bath. Thereafter 15 mL 4 wt% penicillin G potassium salt aqueous solution at 37 °C was added. The mixture was titrated by 0.1 mol L^{-1} NaOH solution to maintain pH value at 8.0. The volume of NaOH solution consumed in the first 10 min was recorded to calculate the specific activity of IMPGA. To ensure the comparability of the specific activity of IMPGA and to avoid the influence of different amount of water contained in the wet IMPGA, the specific activity was calculated by per gram dry IMPGA in this paper.

The specific activity of dry IMPGA was calculated as follows:

$$A(\mathrm{IU\,g^{-1}}) = \frac{V_{\mathrm{NaOH}} \times C_{\mathrm{NaOH}} \times 10^3 \times n}{m \times t}$$

V_{NaOH} (mL) is the volume of NaOH solution consumed; C_{NaOH} (mol L^{-1}) is the concentration of NaOH solution; m (g) is the weight of wet IMPGA; t (min) is the reaction time, i.e. 10 min and n is the weight ratio of wet IMPGA to dry IMPGA.

Another parameter used to characterize the performance of the carrier was the immobilization yield, IMY, which was described as follows:

$$\mathrm{IMY}(\%) = \frac{A_1 - A_2}{A_1} \times 100\%$$

A_1 (IU/mL) is the activity of the enzyme solution before immobilization; A_2 (IU/mL) is the activity of the enzyme solution after immobilization.

The operational stability testing of IMPGA was as follows: after testing the initial specific activity of IMPGA, the solution was separated by centrifugation at 3000 rpm for 5 min, and then the upper liquid was removed quickly, and then the remnant solid was transferred into the reactor to test its specific activity by the same method mentioned above.

2.5. Characterization of APFS

Nitrogen adsorption–desorption isotherms were measured at 77 K with a Micromeritics ASAP 2020M surface area and pore size analyzer. FT-IR spectra were recorded on a Nicolet Nexus 670 FT-IR spectrometer. Thermogravimetry (TG) was carried out on a PerkinElmer Pyris Diamond TG-DTA analyzers, the temperature was heated programmedly from 40 °C to 800 °C at 10 °C/min in the atmosphere of air of 50 mL/min. Solid state ^{13}C and ^{29}Si MAS NMR analysis was performed on a Bruker Avance 500 MHz NMR spectrometers. The TEM images were obtained on a TECNAI 20S-TWIN microscope. The analysis of C, H and N elements was determined by Elementar Vario EL III element analyzer and the amino content of APFS was quantitatively calculated from the N element content.

3. Results and discussion

3.1. Characterization of APFS

3.1.1. FT-IR spectroscopy

Fig. 1 shows FT-IR spectra of APFS samples. Two absorption peaks at 690 cm^{-1} and 1560 cm^{-1}, which were attributed to N–H bending vibration and symmetric NH_2 bending vibration, respectively, were observed clearly and confirmed the presence of amino groups on the silica surface. In addition, the strong absorption peak at 1630 cm^{-1}, which was mainly assigned to N–H bending vibration [24], was overlapped with the bending vibration of absorbed H_2O. The absorption peak of C–N stretching vibration in the range of 1000–1200 cm^{-1} could not be resolved due to its overlap with the absorption peak of Si–O–Si stretching vibration in the range of 1000–1130 cm^{-1} and that of Si–CH_2–R stretching vibration in the range of 1200–1250 cm^{-1} [24,27]. The two absorption peaks at 2934 cm^{-1} and 2879 cm^{-1} attributed to the stretching vibration of –CH_2 groups were clear and the absorption intensities increased with an increase in the volume of APTES in the reaction mixture. The absorption peaks in the range of 3000–3600 cm^{-1} were mainly due to the asymmetric and symmetric stretching vibrations of H_2O and the stretching vibrations of NH_2, therefore, the stretching vibrations of NH_2 in the 3280–3370 cm^{-1} region [28] could not be detected in the samples due to the broad peak centered at 3420 cm^{-1} corresponding to the adsorbed water.

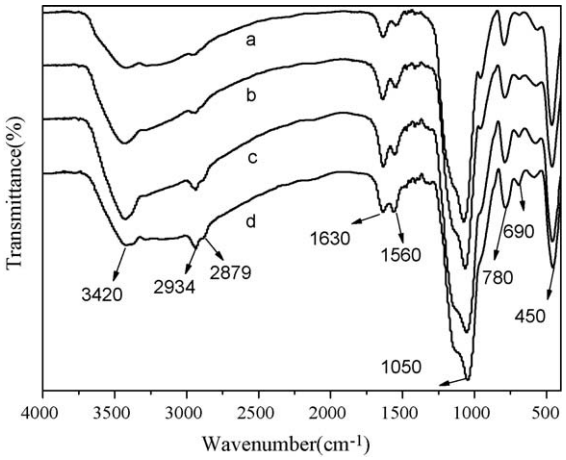

Fig. 1. FT-IR spectra of APFS-*x*-*y* samples: (a) 1–9; (b) 2–8; (c) 3–7; (d) 4–6.

3.1.2. TG

Fig. 2 shows TG profiles of APFS-*x*-*y* samples. All samples showed the first weight loss of 4–8 wt% at the temperatures lower than 130 °C, corresponding to desorption of physically adsorbed water. The second weight loss in the temperature range of 130–300 °C was due to the dehydration reaction between the amino groups and the neighboring surface silanols [29]. The third weight loss in the temperature range of 300–800 °C could be attributed to the decomposition of the aminopropyl groups [24]. With an increase in the volume of APTES in the reaction mixture, the total weight loss in the temperature range of 40–800 °C increased. As shown from Fig. 2, the weight loss of the four samples at the temperature above 300 °C was 13.4 wt%, 16.0 wt%, 19.3 wt% and 22.6 wt% from APFS-1-9 to APFS-4-6, respectively, which confirmed the presence of the aminopropyl groups of the APFS samples.

3.1.3. Element analysis

Table 1 shows element analysis of APFS-*x*-*y* samples. With an increase in the volume of APTES in the reaction mixture, the N or C or H content of APFS-*x*-*y* sample increased, but the actual molar ratio of C/N or H/N in all samples was higher than the theoretical molar ratio in the aminopropyl groups, which could be attributed to CO_2 and H_2O adsorbed on the surface of APFS-*x*-*y* samples only dried at room temperature under vacuum. As shown from Table 1, the maximum amount of amino groups of APFS-*x*-*y* sample could reach to 3.96 mmol g^{-1} and the amount of amino groups increased when increasing the volume of APTES in the reaction mixture.

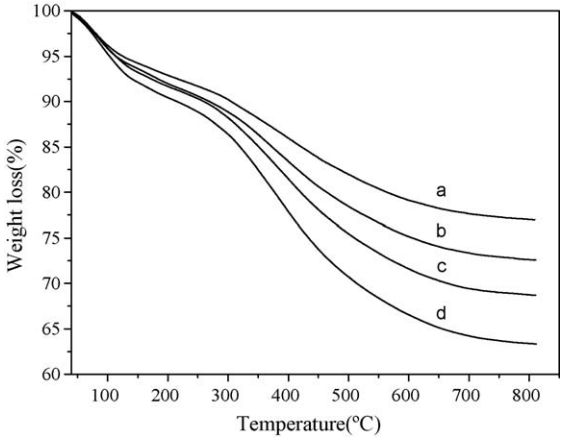

Fig. 2. TG profiles of APFS-*x*-*y* samples: (a) 1–9; (b) 2–8; (c) 3–7; (d) 4–6.

Table 1
Element analysis of APFS-*x*-*y* samples.

Sample	N (wt%)	C (wt%)	H (wt%)	Molar ratio of C/N	Molar ratio of H/N	Total amino amount (mmol g^{-1})[a]
APFS-1-9	2.48	9.66	2.72	4.54	15.35	1.77
APFS-2-8	3.60	12.67	3.30	4.10	12.83	2.57
APFS-3-7	4.40	14.22	3.92	3.77	12.47	3.14
APFS-4-6	5.54	17.12	4.52	3.60	11.42	3.96

[a] The amino content was quantitatively calculated from the N element content.

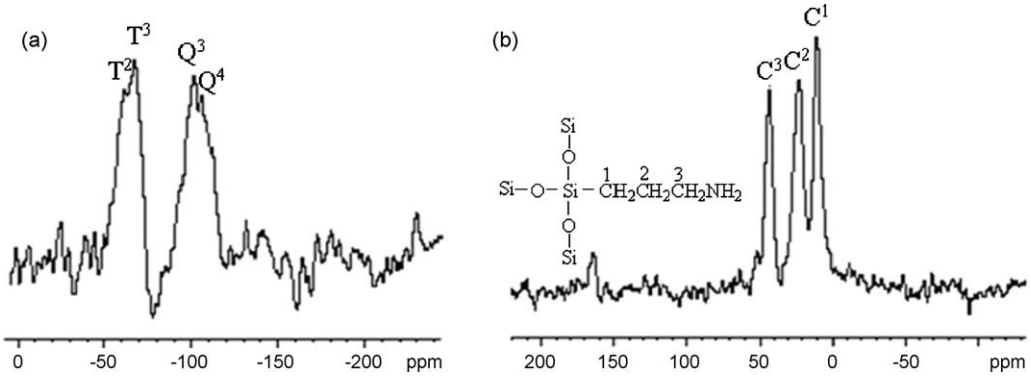

Fig. 3. ^{29}Si MAS NMR (a) and ^{13}C CP/MAS NMR (b) spectra of APFS-4-6 sample.

Furthermore, calculated from the amount of amino groups in Table 1, the weight percentage of the aminopropyl groups of APFS-*x*-*y* samples was 10.3%, 14.9%, 18.2% and 23.0%, respectively, which agreed well with the results determined from TG.

3.1.4. Solid state ^{13}C and ^{29}Si MAS NMR

Fig. 3 shows the solid state ^{29}Si MAS NMR and ^{13}C CP/MAS NMR spectra of APFS-4-6 sample. ^{29}Si MAS NMR spectra in Fig. 3(a) show four distinct resonance peaks, such as two peaks at upper field corresponding to Q^4 ($d = -110$ ppm) and Q^3 ($d = -101$ ppm), and two peaks at lower field assigned to T^3 ($d = -67.5$ ppm) and T^2 ($d = -58$ ppm). The appearance of T^m peaks confirmed that APTES was condensed as the part of the silicate framework. As shown from the ratio of T^m/Q^m in Fig. 3(a), a lot of organic groups were connected with the silicon atoms. ^{13}C CP/MAS NMR spectra in Fig. 3(b) clearly show three resonance peaks at 10.6 ppm, 22.3 ppm and 42.1 ppm, assigned to the C atoms on the Si–CH_2–CH_2–CH_2–NH_2 group in sequence from left to right, respectively [30], which further confirmed that there were lots of aminopropyl groups connected with the silicon. Furthermore, no resonance peaks corresponding to Triton X-100, hexanol and cyclohexane were observed in Fig. 3(b), which indicated that these chemicals were completely removed during washing with acetone.

3.1.5. TEM

Fig. 4 shows TEM images of APFS-*x*-*y* samples with the volume ratio of APTES to TEOS of 0/10, 1/9 and 4/6 in W/O microemulsion. As shown from Fig. 4, with an increase in the volume ratio of APTES to TEOS, the particle began to agglomerate and grow up. The particle size of APFS-0-10 sample was about 10 nm, the particle size of APFS-1-9 sample was about 20 nm, and the particle size of APFS-4-6 sample increased to about 60 nm. The aggregation of APFS-*x*-*y* samples could be due to an increase in the hydrogen bonding interaction among amino groups, which was also reported by Tan and co-workers [31]. During the preparation of APFS-*x*-*y* samples, the reaction mixture was clear in 30 min after adding TEOS. However, when APTES was added, the reaction mixture became milky and was deposited quickly. From this phenomenon, APTES can accelerate the hydrolysis and co-condensation of TEOS and APTES. The amino groups of APTES and ammonium hydroxide can increase pH value of the reaction mixture, which increases the hydrolysis and co-condensation rate. Therefore, the higher the volume ratio of APTES in the reaction mixture is, the faster the reaction rate is. The faster reaction rate and the stronger hydrogen bonding interaction among amino groups make the aggregation phenomenon severer and the particle size bigger.

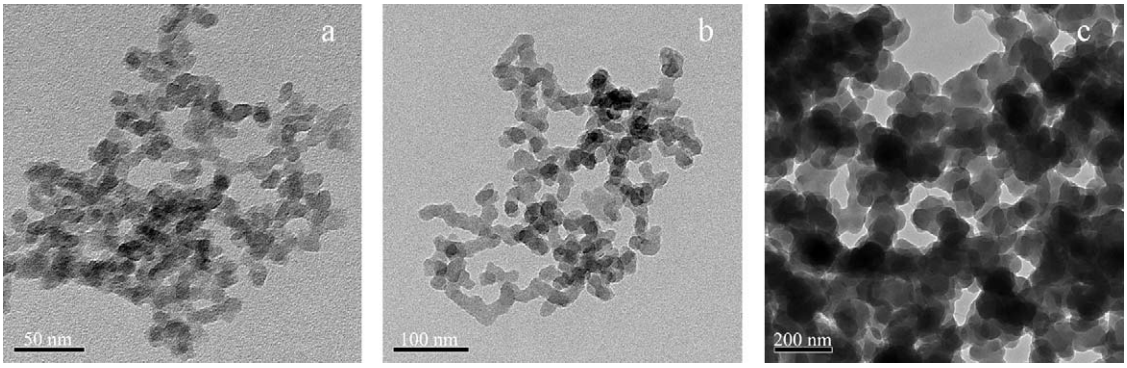

Fig. 4. TEM images of APFS-*x*-*y* samples: (a) 0–10; (b) 1–9; (c) 4–6.

Table 2
Effects of V_{APTES}:V_{TEOS} on the surface area of APFS samples and the performance of IMPGA.

Samples	S_{BET} ($m^2\ g^{-1}$) of APFS	IMPGA		
		Initial specific activity (IU g^{-1})	Operational stability (%)	IMY (%)
APFS-0-10	198	1999	70	85
APFS-1-9	70	2759	86	97
APFS-2-8	58	2369	85	98
APFS-3-7	21	1726	78	54
APFS-4-6	15	1344	83	38

3.2. Performance of IMPGA

Table 2 shows effects of the volume ratio of APTES to TEOS (V_{APTES}:V_{TEOS}) in W/O microemulsion on the surface area of APFS samples and the performance of IMPGA. As shown from Tables 1 and 2, with an increase in V_{APTES}:V_{TEOS}, the amount of amino groups of APFS sample increased obviously, but the surface area of APFS sample decreased dramatically, and the specific activity or the immobilization yield (IMY) of IMPGA increased sharply to a maximum and then declined significantly.

The BET surface area of APFS-0-10 sample (pure silica) was 2.8 times than that of APFS-1-9 sample. The specific activity was 1999 IU g^{-1}, the operational stability was 70%, and IMY was 85% over APFS-0-10 sample, while the specific activity was 2759 IU g^{-1}, the operational stability was 86%, and IMY was 97% over APFS-1-9 sample. PGA is immobilized on APFS-0-10 sample by the hydrogen bonding interaction between amino groups of PGA molecule and the surface silanol groups of the support, however PGA is immobilized on APFS-1-9-G sample mainly by the covalent bonding interaction between amino groups of the enzyme and the surface aldehyde groups of the support, which increases the initial specific activity, the operational stability and the immobilization yield. But the excess surface aldehyde groups of the support results in the multipoint covalent bonding and thus the structure rigidity of PGA molecule, which causes difficulty for the enzyme to induce fit to the substrate [32]. Furthermore, a decrease in the surface area of APFS sample results in a decrease in the surface availability of amino groups. As seen from TEM images of APFS samples in Fig. 4, with an increase in the volume ratio of APTES to TEOS, the particle size of APFS samples increased obviously. Thus most of amino groups of APFS samples were included inside the particles, which were unavailable for PGA immobilization. They result in a decrease in the initial specific activity and IMY. So APFS-1-9 sample is the best support for PGA immobilization.

4. Conclusions

The aminopropyl-functionalized silicas with higher loading of amino groups was synthesized by the one-step co-condensation of TEOS and APTES in W/O microemulsions, and characterized by FT-IR spectroscopy, thermogravimetry, element analysis, solid state ^{13}C and ^{29}Si MAS NMR, TEM, and N_2 adsorption. The results show that the aminopropyl groups were condensed as the part of the silicate framework. Effects of the volume ratio of APTES to TEOS in W/O microemulsion on the physico-chemical properties of APFS sample and the performance of IMPGA were systematically investigated. The suitable surface area and the available amount of amino groups of APFS sample, and covalent bonding interaction are favorable to increase the initial specific activity, the operational stability and the immobilization yield of IMPGA. PGA immobilized on APFS-1-9 sample behaves higher IMY of 97%, higher specific activity of 2759 IU g^{-1} and higher operational stability of 86% after recycled for 5 times.

Acknowledgements

This project was supported financially by the National Basic Research Program of China (2004CB719500), Science and Technology Commission of Shanghai Municipality (06DJ14006) and Special Foundation for Ph.D. Education by Ministry of Education of China (20070251016).

References

[1] A.I. Kallenberg, F. van Rantwijk, R.A. Sheldon, Adv. Synth. Catal. 347 (2005) 905.
[2] G.W. Wuyun, G.Z. Lu, D.Z. Wei, Y.L. Guo, Y.S. Wang, Chin. J. Catal. 24 (2003) 219.
[3] P. Xue, G.Z. Lu, Y.L. Guo, Y.S. Wang, Chem. J. Chin. U 25 (2004) 361.
[4] L.M. van Langen, M.H.A. Janssen, N.H.P. Oosthoek, S.R.M. Pereira, V.K. Švedas, F. van Rantwijk, R.A. Sheldon, Biotechnol. Bioeng. 79 (2002) 224.
[5] M.H.A. Janssen, L.M. van Langen, S.R.M. Pereira, F. van Rantwijk, R.A. Sheldon, Biotechnol. Bioeng. 78 (2002) 425.
[6] J. He, X.F. Li, D.G. Evans, X. Duan, J. Mol. Catal. B 11 (2000) 45.
[7] A.S.M. Chong, X.S. Zhao, Catal. Today 93–95 (2004) 293.
[8] Y.J. Lü, G.Z. Lu, Y.Q. Wang, Y.L. Guo, Y. Guo, Z.G. Zhang, Y.S. Wang, X.H. Liu, Adv. Funct. Mater. 17 (2007) 2160.
[9] P. Xue, G.Z. Lu, Y.L. Guo, Y.S. Wang, Y. Guo, J. Mol. Catal. B 30 (2004) 75.
[10] A. Arkhireeva, J.N. Hay, W. Oware, J. Non-Cryst. Solids 351 (2005) 1688.
[11] X. Zhang, R.F. Guan, D.Q. Wu, K.Y. Chan, J. Mol. Catal. B 33 (2005) 43.
[12] N. Hiyoshi, K. Yogo, T. Yashima, Micropor. Mesopor. Mater. 84 (2005) 357.
[13] X.G. Wang, Y.H. Tseng, J.C.C. Chan, S. Cheng, J. Catal. 233 (2005) 266.
[14] S.G. Wang, Catal. Commun. 4 (2003) 469.
[15] M.P. Kapoor, Y. Kasama, T. Yokoyama, M. Yanagi, S. Inagaki, H. Nanbua, L.R. Juneja, J. Mater. Chem. 16 (2006) 4714.
[16] A.M. Liu, K. Hidajat, S. Kawi, D.Y. Zhao, Chem. Commun. (2000) 1145.
[17] H. Yoshitake, T. Yokoi, T. Tatsumi, Chem. Mater. 14 (2002) 4603.
[18] J. Evans, A.B. Zaki, M.Y. El-Sheikh, S.A. El-Safty, J. Phys. Chem. B 104 (2000) 10271.
[19] H.J. Jm, Y.H. Yang, L.R. Allain, C.E. Barnes, S. Dai, Z.L. Xue, Environ. Sci. Technol. 34 (2000) 2209.
[20] B. Lee, Y. Kim, H. Lee, J. Yi, Micropor. Mesopor. Mater. 50 (2001) 77.
[21] J.F. Dìaz, K.J. Balkus, F. Bediouui, V. Kurshev, L. Kevan, Chem. Mater. 9 (1997) 61.
[22] A.B. Bourlinos, T. Karakostas, D. Petridis, J. Phys. Chem. B 107 (2003) 920.
[23] A. Stein, B.J. Melde, R.C. Schroden, Adv. Mater. 12 (2000) 1403.
[24] A.S.M. Chong, X.S. Zhao, J. Phys. Chem. B 107 (2003) 12650.
[25] X.G. Wang, K.S.K. Lin, J.C.C. Chan, S. Cheng, Chem. Commun. (2004) 2762.
[26] K. Azadeh, K. Farhad, F. Hossein, J. Biosci. Bioeng. 93 (2002) 125.
[27] L.D. White, C.P. Tripp, J. Colloid Interface Sci. 232 (2000) 400.
[28] X. Wang, J.C.C. Chan, Y. Tseng, S. Cheng, Micropor. Mesopor. Mater. 95 (2006) 57.
[29] S.A. Alekseev, V.N. Zaitsev, Chem. Mater. 18 (2006) 1981.
[30] A.S.M. Chong, X.S. Zhao, A.T. Kustedjo, S.Z. Qiao, Micropor. Mesopor. Mater. 72 (2004) 33.
[31] R.P. Bagwe, L.R. Hilliard, W.H. Tan, Langmuir 22 (2006) 4357.
[32] G. Alvaro, R. Fernandez-Lafuente, R.M. Blanco, J.M. Guisan, Appl. Biochem. Biotechnol. 26 (1990) 181.